809
FERMILAB-PROPOSAL-0809

Proposal on the Spin Dependence in Direct-Gamma Production at High $p_\perp$ Using an Upgraded MP Beam Line

LAPP-Annecy, Argonne, Fermilab, Iowa, Kyoto-Kyoto Education-Kyoto Sangyo, Okayama, Osaka Municipal, Los Alamos, Messina, New Mexico State, Northwestern, Rice, CEN-Saclay, IHEP-Serpukhov, INFN-Trieste, Udine*

07 March 1990

Abstract

We propose to study the spin dependence of direct-gamma production at high $p_\perp$ using the MP beam line upgraded from 200 to 500 GeV/c.

The proposed measurements can be carried out primarily using detectors already on hand. The energy upgrade is readily accomplished at a moderate cost using conventional magnets.

Cospokespersons:

A. Masaike (Japan)
S. Nurushev (USSR)
A. Yokosawa

---

* Individual names are likely to be similar to the present participants in E-704. Precise list will be presented later.

Table of Contents

I. Introduction.....1

II. Physics Goals.....2

III. Experimental Setup.....3

IV. Identification of Direct Gamma Events.....5

V. Polarized ^{6}LiD Target.....7

VI. Rate and Error Estimate.....8

VII. Beam Time Request.....9

VIII. Summary.....10

References 11

Figure Captions.....12

Tables 13

Appendix I Energy Upgrade.....16

Appendix II Additional Equipment Needs.....17

I. INTRODUCTION

To understand the basic question of the origin of proton spin, we propose to determine the gluon spin distribution in the proton by measuring the spin correlation parameter A_{LL} in the direct-γ production at high $p_\perp$, with longitudinally polarized protons on longitudinally polarized target nucleons.

Specifically, we propose studies of the spin dependence in direct-gamma production with good statistical accuracy using polarized beams up to 500 GeV/c:

A_{LL} $(p^\uparrow N^\uparrow \rightarrow \gamma + x)$ $p_\perp$ up to 5 GeV/c and

A_N $(p^\uparrow p \rightarrow \gamma + x)$ $p_\perp$ up to 5 GeV/c

The advantages of making the A_{LL} and A_N measurements at higher energies are twofold: i) the direct-gamma production cross section at high $p_\perp$ increases rapidly with energy - from 200 to 500 GeV there is roughly a factor of three increase; and ii) the polarized beam intensity also increases by a factor of three.

The major detector for the direct-gamma measurements will be an electromagnetic calorimeter consisting of 2,448 lead-glass counters. This calorimeter is particularly well-suited for $p_\perp$ coverage from 3 to 5 GeV/c.

To increase the polarized beam energy from the existing 200 GeV/c to 500 GeV/c, an additional eight 4-Q-120 quadrupoles are required. These are in addition to the present configuration of two 4-Q-120's and six 3-Q-120's (to be replaced by 4-Q-120's). Thus a total of fourteen 4-Q-120's will be needed. In a recent study, we found that such a configuration using conventional quadrupoles up to 500 GeV is nearly as effective as the equivalent superconducting quadrupoles originally proposed in 1985. Details on the energy upgrade are shown in Appendix I.

Other experiments, in addition to the one covered in this proposal, including studies of the energy dependence of various reactions studied in E-704 such as: i) $\Delta\sigma_L$(pp and $\bar{p}p$) and ii) asymmetries in π°, η°, Λ/Σ°, $\pi^\pm$ production at large $p_\perp$ or large x_F, are planned. Results obtained during the 1990 fixed-target run at 200 GeV/c should guide our future efforts on these reactions.

II. PHYSICS GOALS

Results of recent experiments to determine the spin-dependent structure function $g_1^p(x)$ of the proton by the EMC group[1] at CERN have been interpreted to mean that the proton spin may not be due to the helicity of its constituent quarks. Instead, most of the proton spin may be due to gluons and/or orbital angular momentum.[2] The spin correlation parameter A_{LL} is approximately proportional to the gluon polarization.[3,4]

The study of double-spin asymmetries can provide quantitative insight into the spin properties of gluons which are not accessible to deep-inelastic ep scattering experiments. The double-spin asymmetry A_{LL} in inclusive direct-γ production has been estimated by several authors.[3,4] The most recent prediction[3] is shown in Section VI together with the proposed measurements.

The QCD Compton effect, "gluon + quark → gamma + quark", is expected to be the dominant mechanism for direct-γ production at large $p_\perp$ at fixed-target energies.

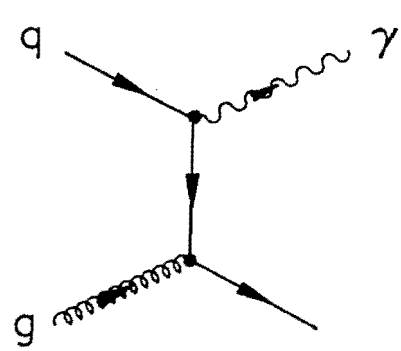

In contrast to the π°, which represents only a fragment of the scattered constituent, the γ itself participates directly in the hard-scattering process. As a direct consequence, the ratio γ/π° should increase with increasing $p_\perp$. This prediction has been confirmed in several different experiments.[5] Thus, direct-γ production provides a particularly clean process for studying the dynamics of hadronic constituents without the complexities of quark fragmentation.

The quantity to be measured is the double-spin asymmetry,

$$A_{LL} = \frac{1}{P_B P_T} \frac{\sigma(++) - \sigma(+-)}{\sigma(++) + \sigma(+-)} ,$$

where ++(+-) indicate parallel (antiparallel) helicities for longitudinally polarized beam (P_B, beam polarization) and target protons (P_T, target polarization). This measurement requires a polarized ^{6}LiD target.

Important qualitative features may also be deduced from single-spin asymmetry measurements. The single-spin asymmetry A_N is expected to be zero, according to perturbative QCD (PQCD).

The quantity to be measured is the single-spin asymmetry

$$A_N = \frac{1}{P_B} \frac{\sigma(\uparrow) - \sigma(\downarrow)}{\sigma(\uparrow) + \sigma(\downarrow)}$$

with a transversely polarized proton beam and liquid hydrogen (H_2) target.

III. EXPERIMENTAL SETUP

Our major attention in the design of the apparatus for the direct-gamma measurement is concentrated in the following areas:

i) Optimize the energy asymmetry, $|E_1 - E_2|/(E_1 + E_2)$, of the two photons from π° and η decays by achieving a sufficient γ-γ separation, low-energy γ detection efficiency, energy resolution, and large acceptance.

ii) Investigate γ-conversion effects in the detectors and target.

iii) Study hadronic shower identification.

A schematic view of the experimental setup is shown in Fig. 1. Trajectories of individual beam particles are defined by hodoscopes H_{B1} and H_{B2} placed upstream and downstream respectively of the snake magnet (see Fig. 1); these are longitudinally separated by 20 meters and have spatial resolutions of 0.9 mm in both the x and y directions. For single-spin measurements an existing liquid H_2 target 100-cm long will be used with the proton beam transversely polarized. For the double-spin asymmetry measurements the longitudinally polarized proton beam will be incident on a longitudinally polarized ^{6}LiD target (for details, see Section V)). The beam polarization will be frequently flipped by the snake magnet as shown in Fig. 1.

Photons produced by the interaction of protons on either a LH_2 or polarized target are detected in the Pb-glass calorimeter (called "CEMC", Central Electromagnetic Calorimeter) consisting of 2,448 Pb-glass cells (3.8 x 3.8 x 45 cm^3) stacked as shown in Fig. 2. The Cerenkov light is collected by a photomultiplier at the rear of each cell. The CEMC is placed 11 m downstream of the target and covers θ = 64.6 mrad which corresponds to $x_F = 0$. The azimuthal angle is fully covered.

The principal characteristics of the CEMC are listed in Table I. This detector has shown remarkable spatial resolution[6] (± 1 mm at 100 GeV), resulting from an optimal choice of tranverse and longitudinal dimensions of the Pb-

glass cells and development of appropriate software for calculating coordinates of the electromagnetic shower using the method of moments.

To accommodate high-event rates, the integrated charge in each cell is digitized by an ADC with pedestal subtraction and energy normalization. Relative gains (PM + ADC) will be monitored with an LED system between spills. The energy resolution has been measured during the last fixed-target run; at full width half-maximum (FWHM) it is

$$\Delta E/E = 0.024 + 0.12/\sqrt{E} \text{ (GeV)}$$

giving ± 2.5% at 25 GeV. Linearity has been studied with electrons from 5 to 100 GeV, and no deviation larger than 1% was observed.

The proportional chambers placed between the target and the CEMC serve to localize charged particles which accompany γ's and assure that there are no charged tracks in the γ direction. To improve background identification in direct-γ production, the CEMC is provided with additional coarse Pb-glass cells as shown in Fig. 2. These additional counters ensure identification, without fine spatial resolution, of π° and η° decays in which only one γ falls within the fiducial area of the CEMC.

With reasonable estimates for processing times we conclude that as many as 500 events/sec can be recorded even at large multiplicities.

IV) IDENTIFICATION OF DIRECT-GAMMA EVENTS

The major background sources involved in the identification of direct-γ's are due to decay events, $\pi^\circ \to \gamma\gamma$ and $\eta \to \gamma\gamma$, where one γ misses a spectrometer, is below threshold for detection, converts in the target, or the two γ's are too closely spaced to be geometrically resolved. Other sources are

due to neutral hadrons such as n, $\bar{n}$, or K_L° interacting in the Pb-glass and thus simulating a single shower (according to Ref. 7, they are negligible). These sources thus give false signals which can be confused with direct-γ's.

These background problems have been investigated using the LUND Monte Carlo (PYTHIA) simulation with the GEANT3 software package. The energy clusters in the CEMC were reconstructed using software developed by the Serpukhov group.[8]

In order to check our simulation procedure, the Monte Carlo calculation was compared to the CERN WA-70 experimental setup[7] in which the $p_\perp$ coverage is similar to the CEMC and $N_{f\gamma}/N_{\pi^\circ}$ generated was 4%, where $N_{f\gamma}$ is the number of faked gamma events (apparent single gammas) and N_{π° is the number of π° events. The calculation was consistent with the actual WA-70 experimental results.

Figure 3 shows the experimental data on the γ-γ separation taken at Serpukhov using the same type of lead-glass counters as those in the CEMC compared with the WA70 results in which lead-scintillator sandwiched counters were used. Figure 4 shows the low-energy γ detection efficiency by the lead glass compared to that of the WA70. Figure 5 shows the π° and η decay asymmetry, $|E_{\gamma_1} - E_{\gamma_2}|/(E_{\gamma_1} + E_{\gamma_2})$, calculated for the CEMC.

A comparison of detector performance between the CEMC and WA70 is shown in Table II.

In Fig. 6, the observed single-γ/π° is shown together with various backgrounds/π° for the lead-glass configuration as shown in Fig. 2. Backgrounds shown in Fig. 6 include:

i) One γ from π° or $\eta \to \gamma\gamma$ misses the detector.

ii) One γ from π° or $\eta \to \gamma\gamma$ is below threshold (0.5 GeV) for detection.

iii) One γ converts in the air, target, etc.

iv) Closely spaced two γ's from π°.

V) Polarized ^{6}LiD Target

It was recently established[9] that substantial nuclear polarizations can be achieved in large targets of ^{6}LiD. To the extent that $^6Li^\uparrow$ can be viewed as He + $D^\uparrow$, as much as one-half of the nucleons are polarized in such a material. Polarizations of $^6Li^\uparrow$ and $D^\uparrow$ approaching 70% should be achievable in the MP-9 polarized target, with the addition of a high-frequency (180 GHz) microwave source.

The special merit of the ^{6}LiD target arises from the much smaller "dilution factor", $1/\alpha$. This quantity $(1/\alpha)$ is related to A_{LL} and ΔA_{LL} as follows:

$$A_{LL} = \varepsilon(\text{raw asymmetry})/\ (P_B \cdot P_T^{eff}),$$

where P_T^{eff} (effective target polarization) = P_T/α and

$$\Delta A_{LL} = \alpha \cdot \Delta\varepsilon/\ (P_B \cdot P_T).$$

P_T is nucleon polarization detected by nuclear magnetic resonance, $1/\alpha = 0.136$ for the present E-704 polarized target, $C_5H_{12}O$, and $1/\alpha = 0.50$ for the ^{6}LiD target. In terms of the running time required, there is a factor of $(.50/.136)^2 \approx 14$ reduction. We also have less background from an "unpolarized" target nucleus.

VI RATE AND ERROR ESTIMATE

Rates for γ production have been estimated with the following assumptions:

Primary Beam:	$4 \cdot 10^{12}$ incident protons/spill (The amount was based on the present Tevatron condition)
Beam Momentum:	450 GeV/c
Beam Intensity:	8.0×10^7/spill with 1 spill/60 sec, and beam polarization, $P_B = 0.45$
γ-Conversion Losses:	In the polarized target and air are 15% and 5% respectively
Liquid H_2 target:	100-cm long for A_N measurements
Polarized ^{6}LiD target (He + $2p^\uparrow$ + $2n^\uparrow$):	20-cm long for A_{LL} measurements

1) A_N Measurement

The invariant cross section for π° production was calculated with the parametrization of R. M. Baltrusaitis et al.[10],

$$f = E(d^3\sigma/d^3p) = A \cdot p_\perp^{-N} (1 - x_R)^M,$$

where $x_R = (x_F^2 + x_\perp^2)^{1/2}$, $A = 2.91 \cdot 10^{-27}$ cm^2/GeV^2, $M = 4.94$, $N = 8.79$.

For the direct-γ production, the ratio γ/π° has been referred to the WA-70 results.[7] The direct-γ events for 500 hours of useful beam time are shown in Table II.

The statistical error in A_N is $\Delta A_N = \sqrt{\chi}\ /(P_B \cdot \sqrt{N_{Tot}})$, where χ is the ratio of total single-γ events over direct-γ events. Statistical errors are shown in Table II with respect to the $p_\perp$ coverage.

2) A_{LL} Measurment

The raw asymmetry for direct-γ production is related to the total asymmetry, ε_{LL}^{Tot}, and the faked γ asymmetry, $\varepsilon_{LL}^{f\gamma}$, as

$$\varepsilon_{LL}^{\gamma} = \alpha\ \chi\ \varepsilon_{LL}^{Tot} - (\chi - 1)\varepsilon_{LL}^{f\gamma},$$

where α is the ratio of all nucleons over polarized nucleons in the target and $\varepsilon_{LL}^{f\gamma}$ can be obtained by π°, η measurements (E-704). The statistical error, $\Delta\varepsilon_{LL}^{\gamma}$, may be approximated as

$$(\Delta\varepsilon_{LL}^{\gamma})^2 = (\alpha\ \chi)^2\ (\Delta\varepsilon_{LL}^{Tot})^2 + (\chi - 1)^2\ (\Delta\varepsilon_{LL}^{f\gamma})^2\ ,$$

where $\Delta\varepsilon_{LL}^{Tot} = (N_{Tot})^{-1/2}$.

$$\Delta A_{LL}^{\gamma} = \Delta\varepsilon_{LL}^{\gamma}/(P_B \cdot P_T).$$

In Table III, for a run of 2500-hour estimates of statistical errors in A_{LL}^{γ} are shown. The second term in the $\Delta\varepsilon_{LL}^{\gamma}$ will be much smaller than the first term and is neglected in ΔA_{LL} estimates.

Statistical error for the direct-γ production is compared with predictions[3] as shown in Fig. 7.

VII) Beam Time Request

We will be ready to carry out these measurements during the next fixed-target period (1992).

Machine Time:

1)	500-GeV beam tuning	100 hours
2)	Calibration	100 hours
3)	A_N	500 hours
4)	A_{LL}	2500 hours

Summary

$A_{LL}(p^{\uparrow}N^{\uparrow} \rightarrow \gamma\ x)$ measurements at high $p_{\perp}$ are sensitive to the gluon spin distribution in proton. The direct-gamma production channel is the best and most efficient measurement for this purpose among other possibilities. This type of experiment can be performed only at Fermilab because of the unique polarized beam facility.

In addition, A_{LL} $(p^{\uparrow}N^{\uparrow} \rightarrow \pi^{\circ}x)$ data will simultaneously be obtained together with direct-gamma data. This channel also offers important information regarding the gluon spin distribution.

REFERENCES

1) J. Ashman et al., Phys. Lett. B206, 364 (1988); Nucl. Phys. B328, 1 (1989).

2) S. J. Brodsky, J. Ellis, and M. Karliner, Phys. Lett. B206, (1988) 309 CERN preprint EP/89-73 (1989).

3) E. L. Berger and J. W. Qiu, Phys. Rev. D40, (1989) 778; D40, (RC) (1989) 3128.

4) M. B. Einhorn and J. Soffer, Nucl. Phys. 274, 714 (1986); N. S. Craigie, K. Hidaka, M. Jacob, and F. M. Renard, Phys. Reports, 99, 143 (1983), and references therein.

5) For instance, see A. Bernasconi et al., Phys. Lett. 206, 163 (1988).

6) F. Binon et al., Nucl. Instr. Meth., A248, 86 (1986).

7) M. Bonesini et al., Z. Phys. C37, 39 (1987); Z. Phys. C38, 371 (1988).

8) Yu. A. Matulenko et al., IHEP 82-29, Serpukhov, E-112 (1982).

9) P. Chaumette et al., Proceedings of the Symposium on High Energy Spin Physics, Minneapolis, Minnesota, September, 1988.

10) R. M. Baltrusaitis et al., Phys. Rev. Lett. 44, 122 (1980).

FIGURE CAPTIONS

Figure 1 Schematic view of the experimental arrangement.

Figure 2 Lead-glass array in the direct calorimeter. The inner calorimeter called "CEMC", central electromagnetic calorimeter, consists of 2.448 Pb-glass cells (38 x 38 x 450 mm^3). The outer calorimeter (surrounding counters) consists of 196 Pb-glass cells (114 x 114 x 300 mm^3).

Figure 3 π° reconstruction efficiency vs. γ-γ distance from WA70 results[7] and Serpukhov results.[8].

Figure 4 γ detection efficiency vs. E_γ from WA70[7] and Serpukhov[8] results.

Figure 5 γ-energy asymmetry $p_\perp > 3.5$ GeV/c; (a) π°, (b) η.

Figure 6 Single-γ observed and backgrounds. Solid: total single-photon events/π° generated. Dotted: total fake-photon background/π° generated. Dotted-Dashed: fake-photon background from π°/π° generated. Double Dot-Dashed: fake-photon background from η/π° generated.

Figure 7 Predicted asymmetry A_{LL} as a function of $p_\perp$ at $x_F = 0$ in $p^\uparrow D^\uparrow$ interactions at $p_{lab} = 400$ GeV/c. Statistical error at $p_\perp = 4$ GeV/c is shown. The solid and dashed curves correspond to parameter choices $x_c = 0.2$ and 1.0 respectively, where a simple one parameter function which satisfies both the large x and small x constraints for $\Delta G\ (x, Q_0^2)$ is selected as[3]:

$$\Delta G(x, Q_0^2) = \begin{cases} G(x, Q_0^2), & x_c \le x \le 1 \\ \frac{x}{x_c} G(x, Q_0^2), & 0 \le x \le x_c. \end{cases}$$

Figure 8 Polarized beam intensity vs. momentum.

Table I

Parameters and Characteristics of the CEMC and Surrounding Calorimeters

	CEMC	Surrounding Calorimeter
- Lead-glass cell dimensions	38 x 38 x 450 mm^3	114 x 114 x 300 mm^3
- Type of glass	TF1-000	SF-6
Radiation length	18	18
- Total number of cells	2448	196
- Working area and weight of the spectrometer	3.6m^2, 50 t	2.6m^2, 6.8 t
- Photomultiplier	FEU-84-3	R1911-05
- Mass resolution for decaying particles	± 8%	± 20%
- Time resolution	~ 100 nsec gate	~ 100 nsec gate

Table II

Comparison of CEMC and WA70

	2γ Separation (for 80% Efficiency) (mm)	Low Energy γ Threshold (GeV)	E_γ Resolution $\Delta E/E \approx C/\sqrt{E}$	$p_\perp$ Coverage (GeV/c)
WA70	15	0.5	C = 0.40	4 ~ 6
CEMC	25	< 0.5	C = 0.12	3 ~ 6

TABLE III

A_N

$p_\perp$ (GeV/c)	$\langle p_\perp \rangle$	$\langle X_\perp \rangle$	$\Delta p_\perp$	Δx_F	n	ΔA_N
2.8 - 3.3	3.0	0.23	0.5	0.21	4.0×10^5	± .021
3.3 - 3.8	3.5	0.26	0.5	0.20	1.4×10^4	± .029
3.8 - 4.3	4.0	0.29	0.5	0.19	4.8×10^3	± .044
4.3 - 4.8	4.5	0.33	0.5	0.18	2.1×10^3	± .061
4.8 - 5.3	5.0	0.36	0.5	0.18	9.8×10^2	± .087

Table IV

A_{LL}

$p_\perp$ (GeV/c)	$\langle p_\perp \rangle$	$\langle X_\perp \rangle$	$\Delta p_\perp$	Δx_F	n	ΔA_{LL}
2.8 - 3.3	3.0	0.23	0.5	0.21	5.7×10^5	± .018
3.3 - 3.8	3.5	0.26	0.5	0.20	2.0×10^5	± .025
3.8 - 4.3	4.0	0.29	0.5	0.19	6.8×10^4	± .037
4.3 - 4.8	4.5	0.33	0.5	0.18	3.0×10^4	± .052
4.8 - 5.3	5.0	0.36	0.5	0.18	1.4×10^4	± .074

APPENDIX I

Energy Upgrade

Some studies of upgrading the MP beamline with conventional quadrupoles instead of superconducting (originally proposed several years ago) were carried out by D. G. Underwood at Breckenridge (summer 1989). We note that the original beam design had room for four 10-foot quadrupoles at each station and we have only two quads at each station presently. Therefore altogether we can have 16 of the 4-Q-120 for the energy upgrade. The maximum momentum obtainable is close to 500 GeV/c and the flux is about three times what we have achieved at 185 GeV/c, as shown in Fig. 8. The electrical cost estimate was made by the Research Division ($94K).

APPENDIX II

Additional Equipment Needs

			Provider
1)	Additional CEMC Counters (already in)		Serpukhov
2)	Surrounding Calorimeters	196 lead-glass counters ~ $300K	Kyoto, Argonne
3)	PC-4 (see Fig. 1)		Iowa, Trieste
4)	Polarized Target Related	Holding coil	Argonne, Saclay
		Microwave source	Argonne, Kyoto, Saclay
5)	PREP Items	ADC's HV supplies	

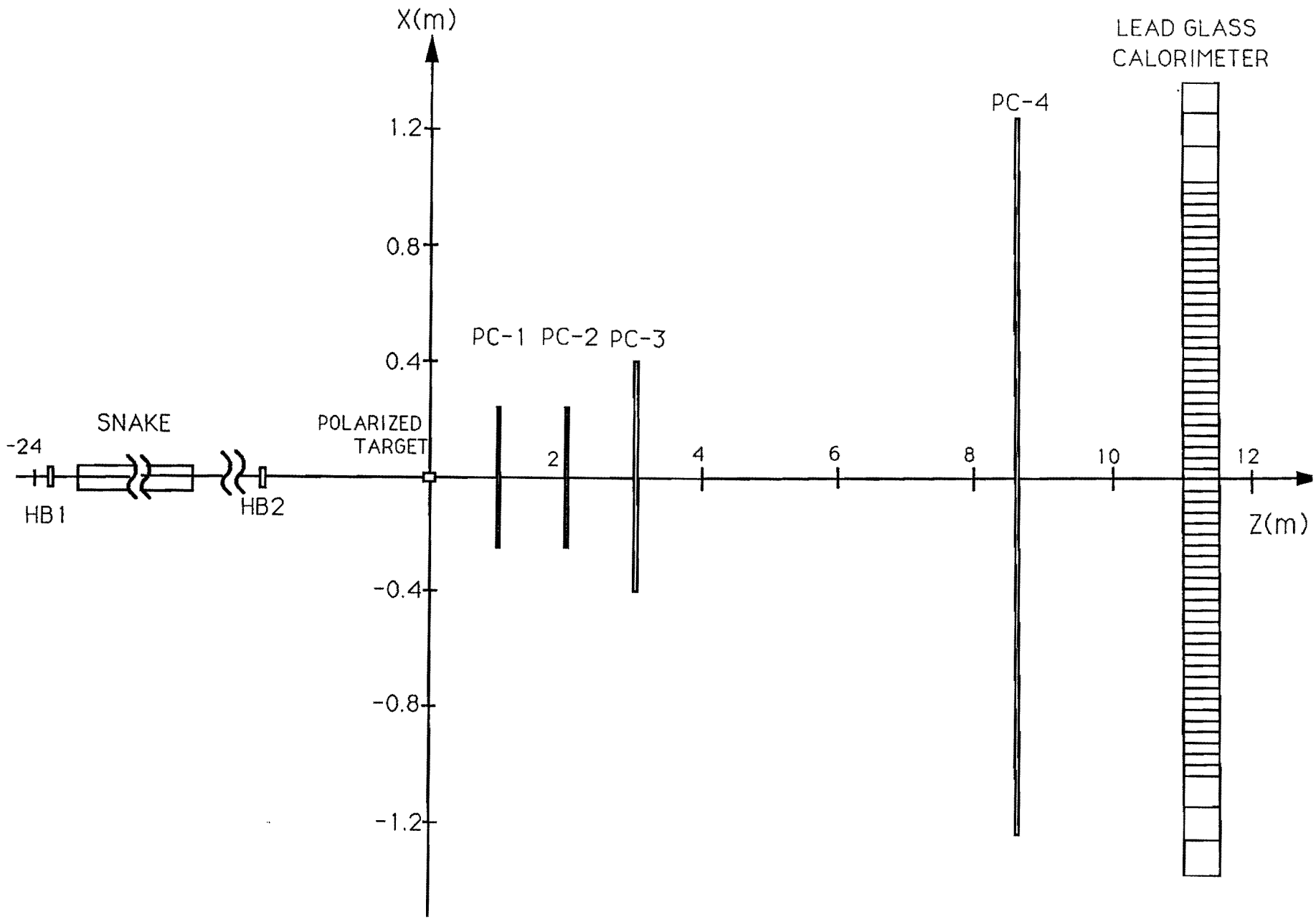
X(m)
1.2
0.8
0.4
-0.4
-0.8
-1.2
LEAD GLASS
CALORIMETER
PC-4
PC-1
PC-2
PC-3
SNAKE
-24
HB1
HB2
POLARIZED
TARGET
2
4
6
8
10
12
Z(m)

Figure 1

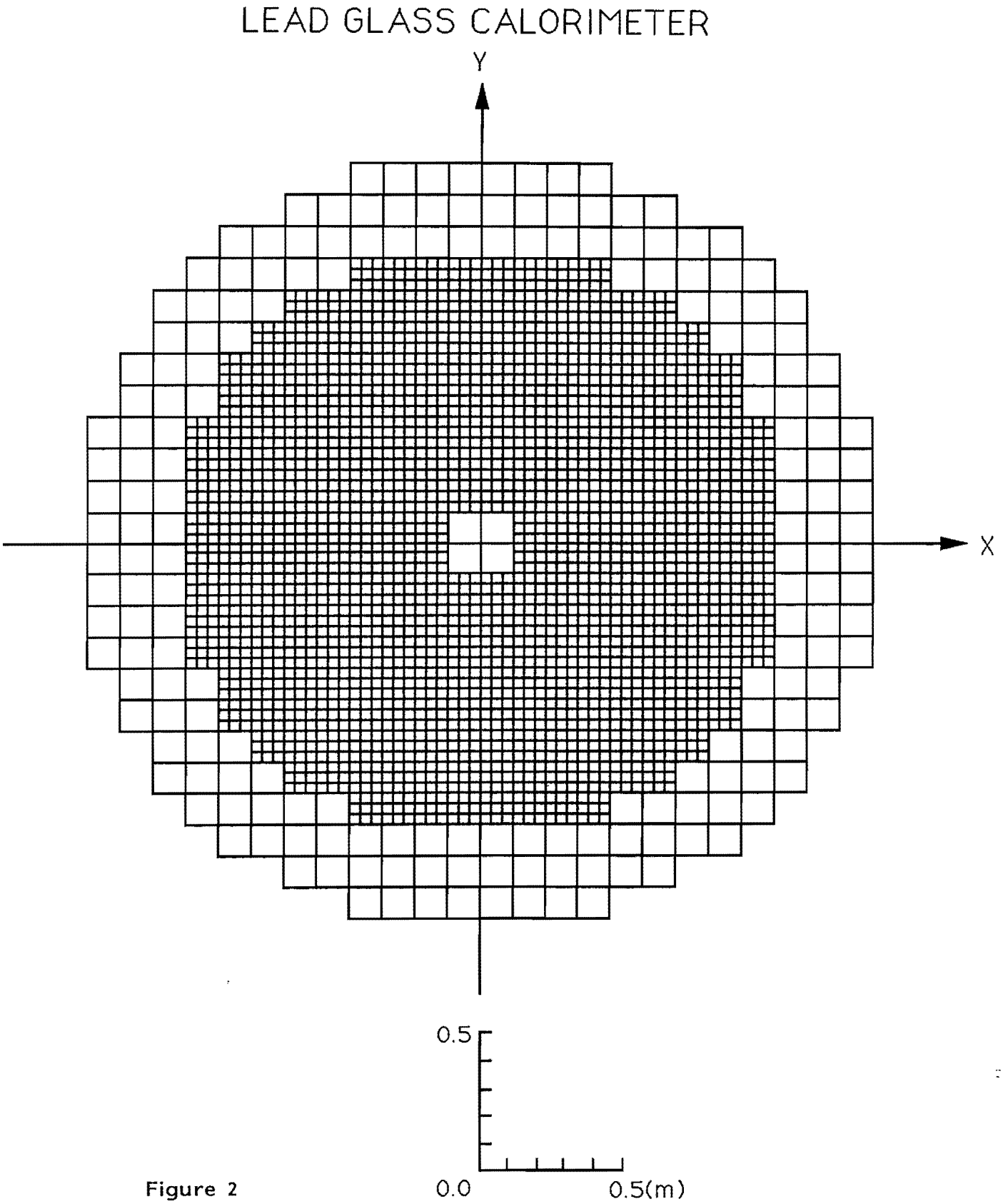

Figure 2

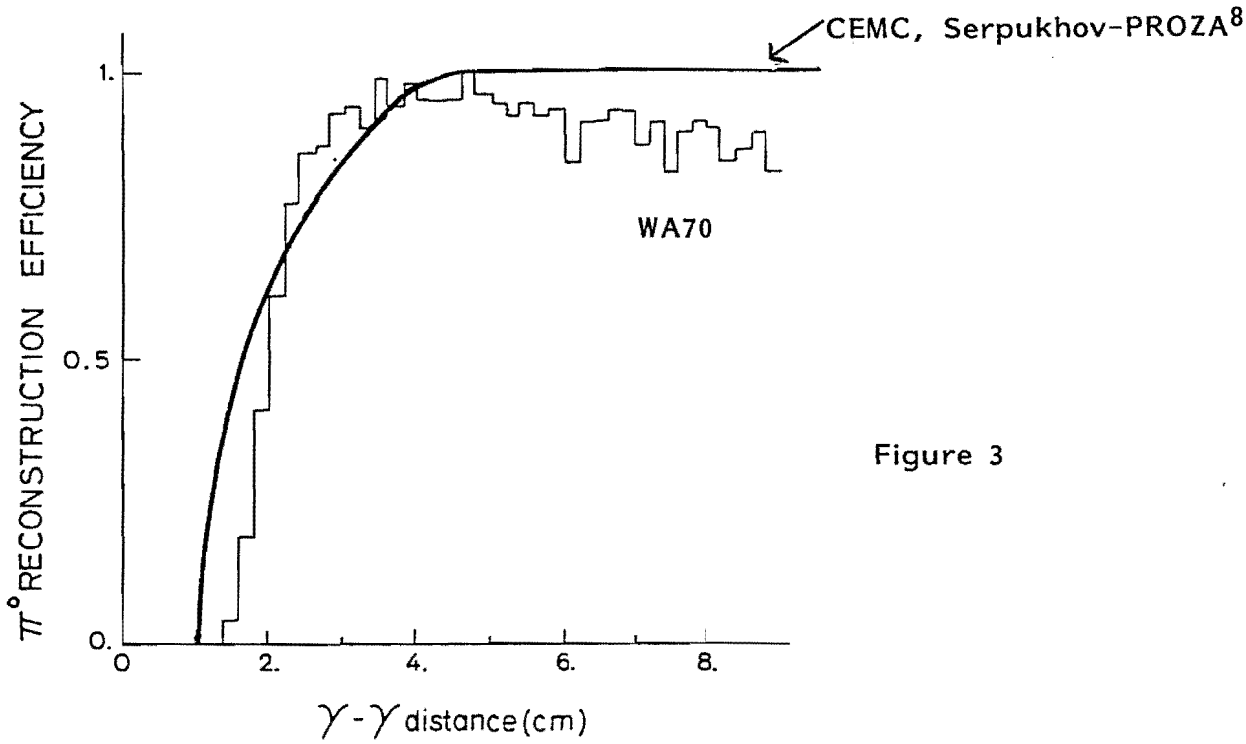

Figure 3

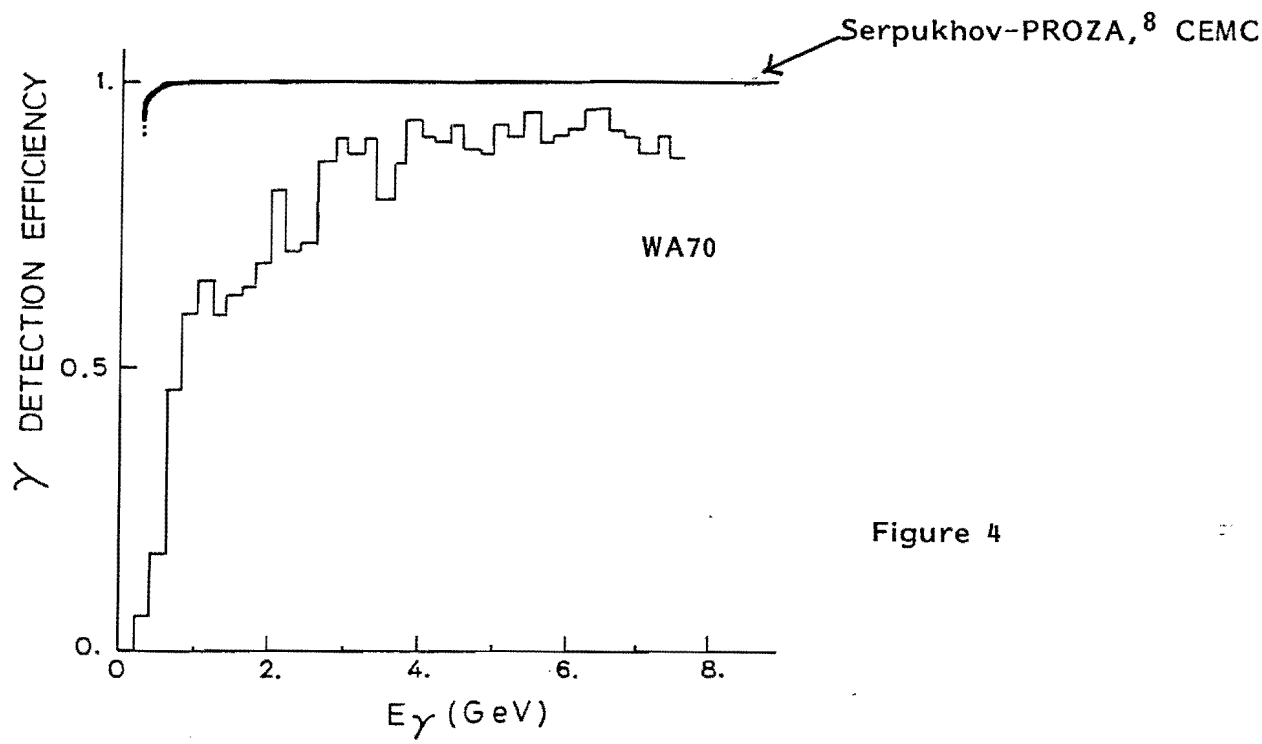

Figure 4

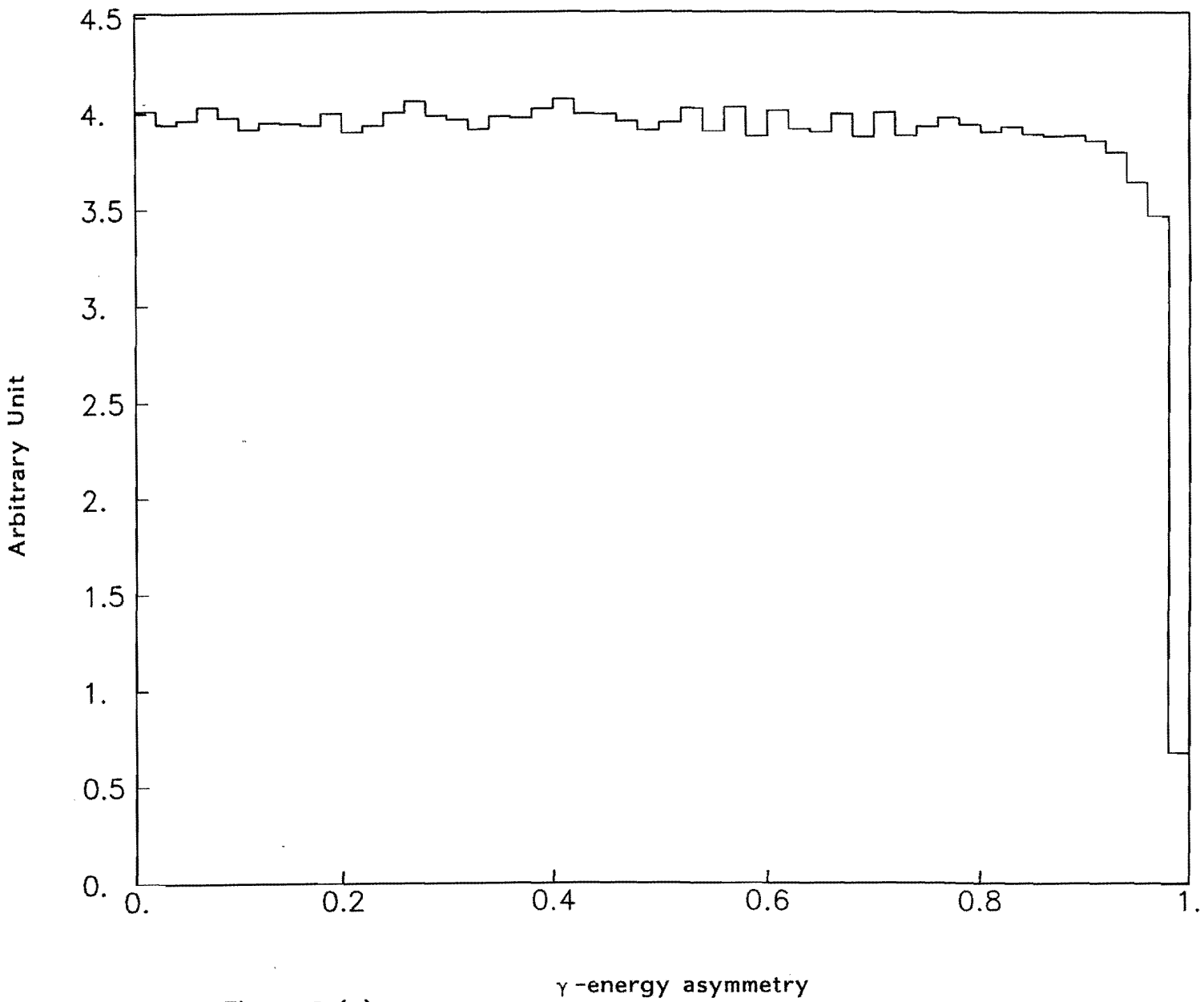
4.5
4.
3.5
3.
2.5
2.
1.5
1.
0.5
0.
Arbitrary Unit
0.
0.2
0.4
0.6
0.8
1.
γ -energy asymmetry

Figure 5 (a)

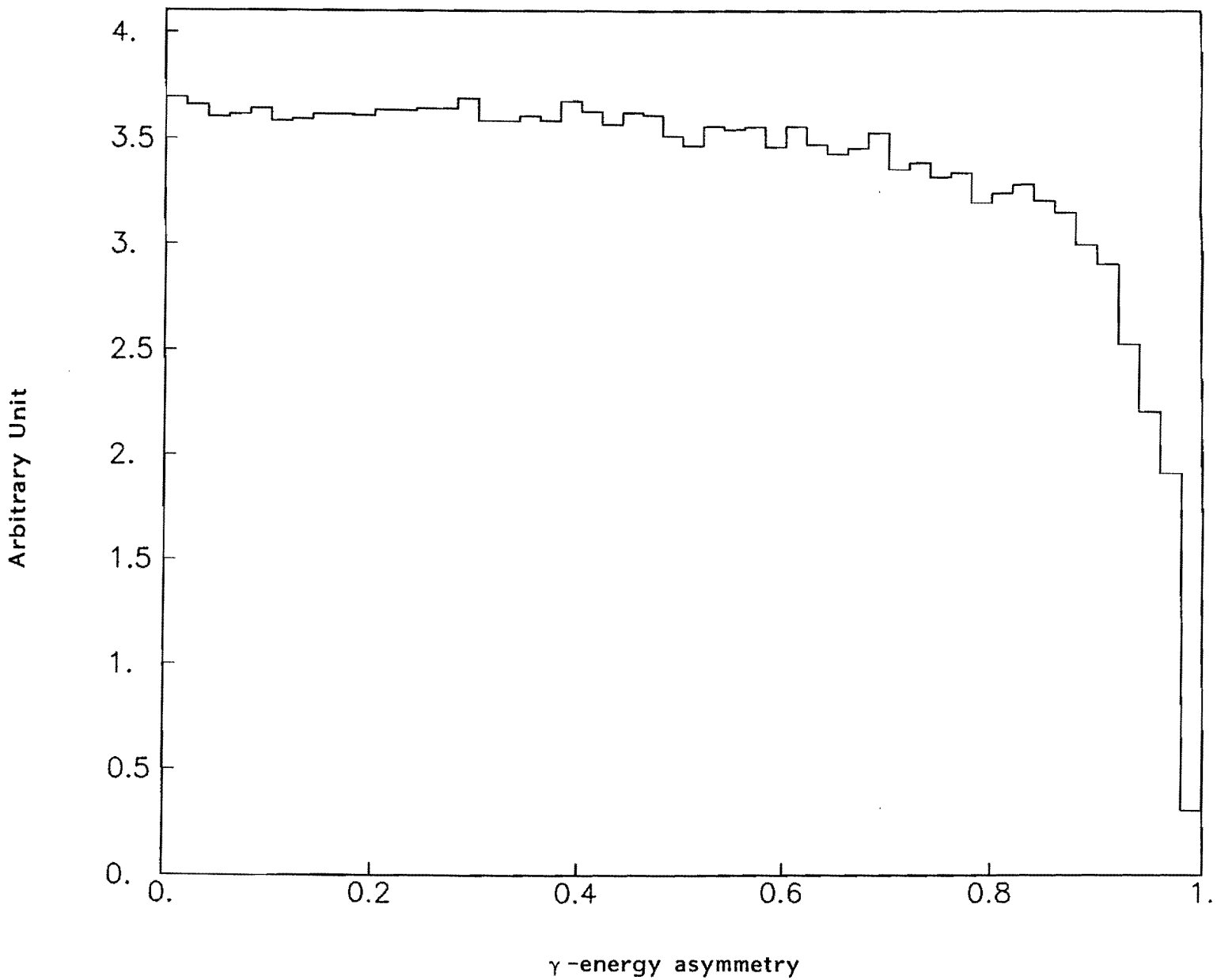
4.
3.5
3.
2.5
2.
1.5
1.
0.5
0.
Arbitrary Unit
0.
0.2
0.4
0.6
0.8
1.
γ -energy asymmetry

Figure 5(b)

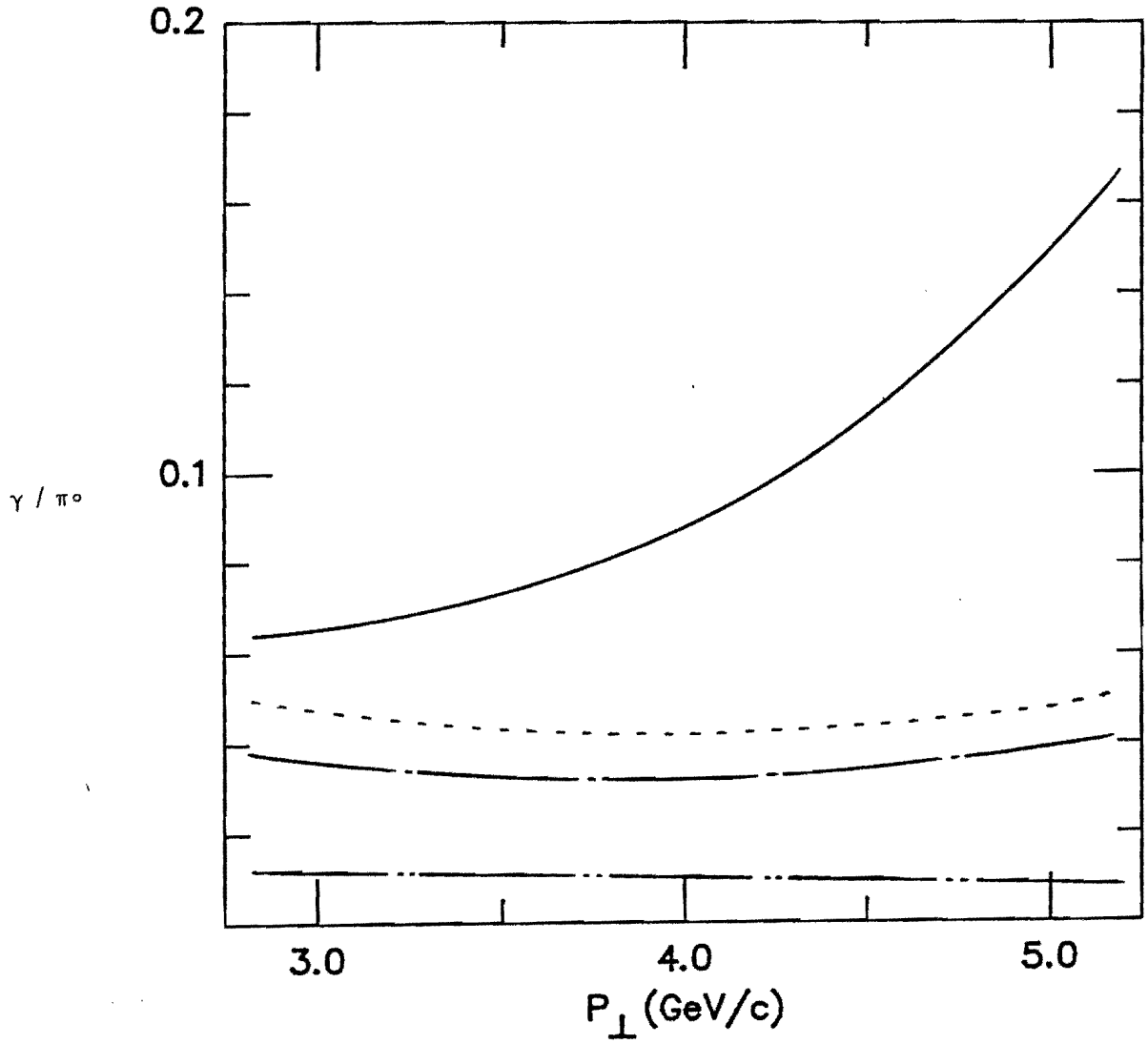

Figure 6

03246

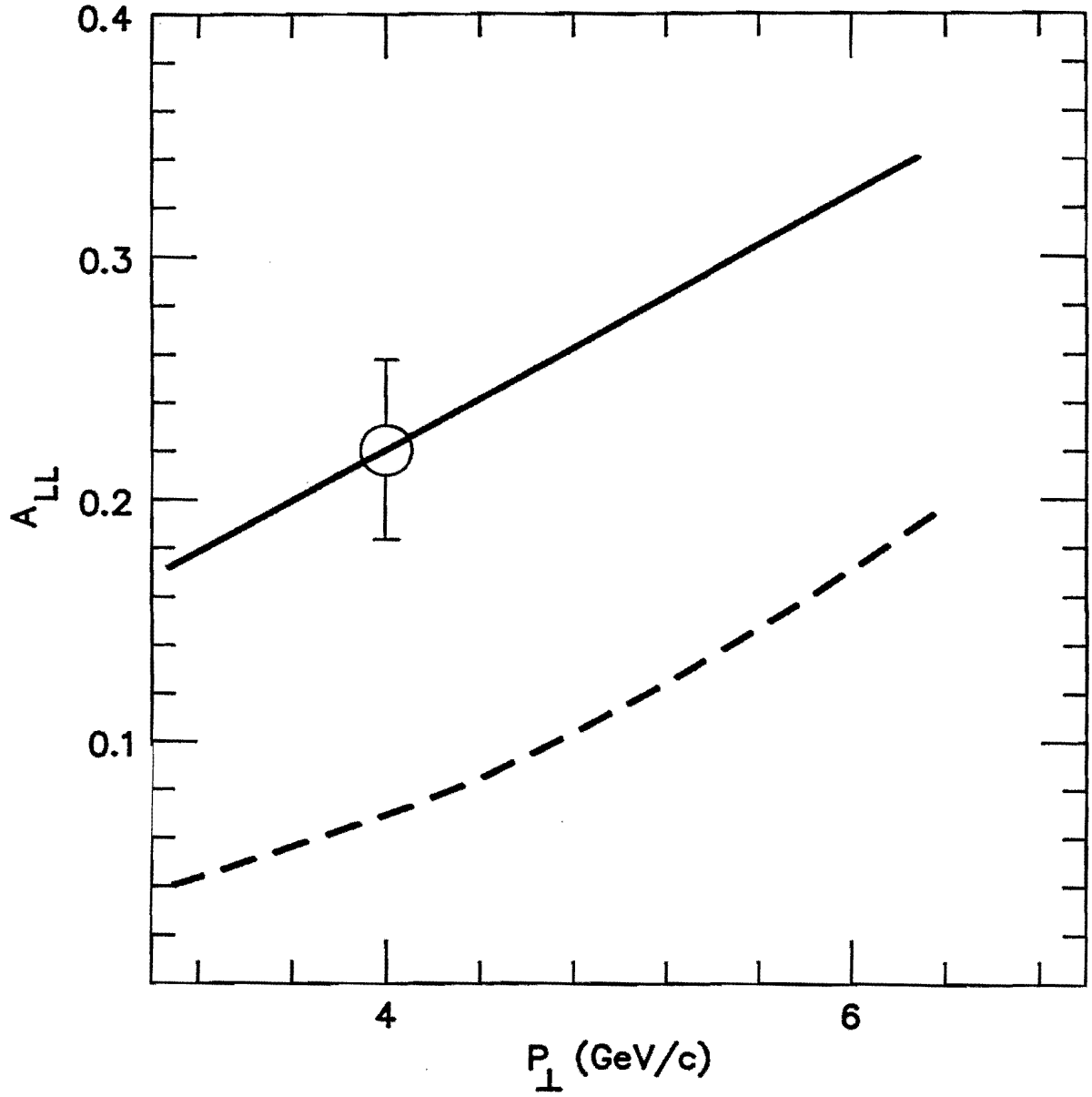

Figure 7

03245

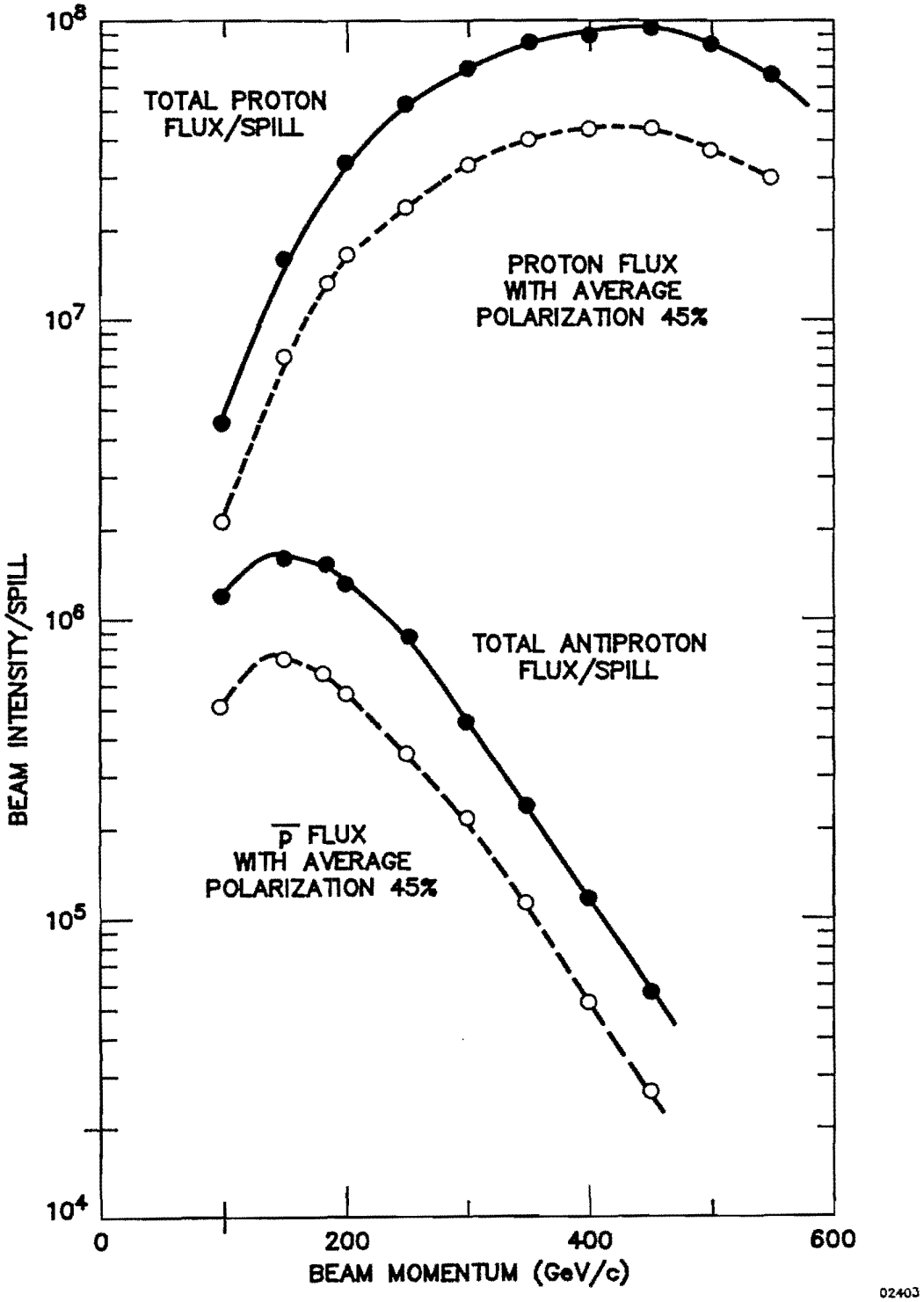
TOTAL PROTON
FLUX/SPILL
PROTON FLUX
WITH AVERAGE
POLARIZATION 45%
TOTAL ANTIPROTON
FLUX/SPILL
$\overline{p}$ FLUX
WITH AVERAGE
POLARIZATION 45%
BEAM INTENSITY/SPILL
10^8
10^7
10^6
10^5
10^4
0
200
400
600
BEAM MOMENTUM (GeV/c)
02403

Figure 8